

## **Ion microprobe techniques and analyses of olivine and low-Ca pyroxene**

I. M. STEELE, R. L. HERVIG, I. D. HUTCHEON AND J. V. SMITH

*Department of Geophysical Sciences, University of Chicago  
Chicago, Illinois 60637*

### **Abstract**

Experimental conditions for major, minor, and trace element analysis of olivine and low-Ca pyroxene are described and analytical accuracy tested using suites of natural samples spanning a wide range of Mg/Fe.

Special attention was given to sample cleanliness to avoid contamination, instrumental vacuum to eliminate hydrides in the secondary ion spectrum, and sample preparation to give good precision in measured intensities. Especially bothersome were molecular interferences in the secondary ion spectrum which were separated from analytical peaks using mass resolution ( $M/\Delta M$ ) over 3000. Careful analysis of the secondary ion spectrum allowed choice of either high or low mass resolution depending on the presence of interferences. Lithium (0.005), F (?), Na (0.01), Mg, Al (0.1), Si, P (5), K (0.05), Mn (0.1), Fe, and Co (1) were analyzed at low resolution with detection limits (ppm) in parentheses. Elements requiring high resolution include Ca (1), Sc (1), Ti (1), V (1), Cr (1) and Ni (5).

The secondary-ion intensities for Mg and Si do not correlate linearly with composition whereas Fe is nearly linear. The simple relation of the Mg/(Mg + Fe) ratio to the measured secondary ion ratio  $Mg^+/(Mg^+ + Fe^+)$  enabled major element determination to within  $\pm 1$  mol% of forsterite or enstatite content. The yield of Mg and Fe secondary ions is a complex function of composition, and  $Mg^+/Si^+$  and  $Fe^+/Si^+$  are not simply related to atomic ratios in the target.

To test accuracy of minor element determination as a function of major element variation, secondary-ion intensities were compared with compositions based on electron probe measurements. Some elements (Al, Cr, Ti, Mn) give a linear relationship with no obvious matrix effect, but Ni, and possibly Ca and Co, definitely depend on the matrix. The linear relationship allows composition determination to within  $\pm 10\%$  of the amount present by reference to known standards. A major effort is required to calibrate Li, K, Na, F, V and Sc for which few reliable standards exist.

### **Introduction**

The development of the electron microprobe in 1960-1970 brought about a revolution in the study of rocks and minerals: indeed, it could be called a "chemical microscope" because rapid non-destructive analyses became possible at spots selected by optical study. It was no longer necessary to separate minerals for analyses of major and minor elements with atomic number ( $Z$ ) greater than 10, and chemical zoning could be studied with a spatial resolution near  $1 \mu m$ . However, light elements could not be analyzed, and the continuous X-ray spectrum placed a detection limit near 40 ppm ( $2\sigma$ ) for elements with  $Z > 10$ . Many techniques (*e.g.*, spark-source and isotope-dilution mass spectrometry; neutron activation

analysis) are available for analysis of trace elements, but most of them require mechanical separation of the material to be analyzed. The ion microprobe was recognized around 1970 to be a potential "chemical microscope" for many trace elements, and qualitative analyses rapidly became routine especially in the study of metals and doped semiconductors. Quantification of analyses of materials has posed severe practical and theoretical problems. Although these problems are not fully solved, we now describe analytical techniques for reliable ion microprobe analyses of various trace elements in olivine and low-Ca pyroxene. Particular emphasis is placed on the use of high mass resolution for identification and separation of mass interferences.

The ion microprobe utilizes a focused primary ion

beam to sputter a small volume of material from a target; some sputtered atoms are ionized and these secondary ions (SI) are analyzed with a mass spectrometer. The extremely low background in a SI mass spectrum allows analysis of trace elements, and the focused beam can be positioned carefully on the sample surface. Although the potential of this analytical technique has been discussed (*e.g.*, Evans, 1972; Liebl, 1975; Werner, 1975), relatively little has appeared regarding its potential for analysis of geological materials. To provide a fundamental test of the technique with typical applications, we have embarked on a systematic study of important rock-forming minerals using an AEI IM-20 ion probe with high mass-resolution (Banner and Stimpson, 1975). These specific studies follow several years devoted to instrument development and to practical experience in analysis of geologic samples.

By far the greatest hindrance to measurement of raw SI intensity data are molecular interferences which often are far more intense than an analytical peak. For example, in mafic silicates  $^{24}\text{Mg}^{16}\text{O}^+$  occurs at the same nominal mass (= 40) as the most abundant Ca isotope. Thus measurement with a mass resolution sufficient only to separate adjacent nominal masses will give incorrect intensity data.

Two contrasting techniques are currently available to reduce the effects of molecular interferences. Herzog *et al.* (1973) and Shimizu *et al.* (1978) described application of energy filtering to increase the signal to interference ratio while Bakale *et al.* (1975) and Steele *et al.* (1980) described use of high mass resolution to separate analytical peaks from interferences. Because the AEI IM-20 ion microprobe allows only limited energy filtering (Steele *et al.*, 1977a), we prefer to use high mass resolution when interferences are present.

The precision and accuracy of measurements is crucial to use of the ion microprobe. Central thereto is the influence of the mineral matrix on the sputtered ion intensities and any systematic instrumental effects. To attempt to answer this question we assembled a suite of natural samples of olivine and low-Ca pyroxene to span nearly the entire range of Mg/Fe. After careful electron-probe analysis for all detectable elements we systematically examined the SI spectrum to determine analytical conditions for each element as well as other elements not detected with the electron probe. We then compared ion-probe count rates against electron-probe measurements to test the quantitative ability of the ion-probe technique.

### Sample selection and preparation

Natural olivines lie very close to the binary join  $(\text{Mg,Fe})_2\text{SiO}_4$ , but several elements including Ni, Ca and Mn are at high enough levels for comparison of ion and electron probe analyses. Low-Ca pyroxenes lie fairly close to the binary join  $(\text{Mg,Fe})\text{SiO}_3$  and several elements, especially Al, Ca, Mn, Cr and Ti are readily measured with an electron microprobe. Chemically-analyzed low-Ca pyroxenes were used by Howie and Smith (1966) to test correction procedures for the electron microprobe, and a selected suite of these pyroxenes was mounted for ion probe analysis. Olivines were selected from those analyzed by Simkin and Smith (1970) and Smith (1966). Several other homogeneous olivines were used as well as an extensive suite of Mg-rich olivines and orthopyroxenes from mantle-derived peridotites which had been carefully analyzed with the electron probe (Hervig, 1980). Choice of samples was based mostly on grain size and absence of visual inclusions. Because only six one-inch diameter samples can be placed in the sample chamber of the ion probe and because rapid sample exchange is not feasible if vacuum is to be maintained at  $<10^{-8}$  torr, grain mounts with up to 36 samples in each sample holder were prepared. A second important consideration in choosing this mounting method is that the relative ion intensities appear to be sensitive to the physical environment (holes, cracks, *etc.*) in the vicinity of the analysis point; thus a rather large insulating surface with few defects is required. Sample mounts were prepared by scribing a grid of 2 mm squares on one side of a 1-inch diameter fused silica disk in a  $6 \times 6$  array. A thin layer of epoxy was placed on the non-scribed side of the silica disk, and grains were placed within individual squares during observation with transmitted light under a stereomicroscope. Each grain was checked for visual defects while in the epoxy, and removed if necessary. With practice, 36 samples each of ~5 grains were mounted in a two hour period. Each mount was ground to thin-section thickness and polished. To avoid possible surface contamination (see below), diamond polishing compound was made by mixing graded diamond powder with commercial "vaseline". All commercial diamond pastes were found to have high levels of K, Na, Cl, Si, F, Ca and other elements. Commercial vaseline was found to be contaminant-free at detection levels of the electron microprobe. Because of possible hydrocarbon contamination and degassing under high vacuum, thick epoxy mounts were not used;

standard thin sections do not noticeably degrade the vacuum. A reflected light photograph was taken of each sample and any particular features such as inclusions and exsolution lamellae were noted.

Before analysis by the ion probe, selected grains of each sample were analyzed with an ARL-EMX-SM electron probe. Operating at 25 kV, with a high beam current (2 $\mu$ A) and a spot diameter ( $\sim$ 25 $\mu$ m) comparable to that of the ion probe, analyses for major elements as well as Na, Al, Ca, Ti, Cr, Mn and Ni were obtained for both olivines (Table 1) and pyroxenes (Table 2) with detection levels (2 $\sigma$ ) below 100 ppmw. Standards used were Ca<sub>2</sub>P<sub>2</sub>O<sub>7</sub> (66.9 wt.% P<sub>2</sub>O<sub>5</sub>), Corning V glass (0.80 wt.% TiO<sub>2</sub>, 0.76 wt.% Cr<sub>2</sub>O<sub>3</sub>), diopside<sub>85</sub>-jadeite<sub>15</sub> glass (22.0 wt.% CaO, 3.78 wt.% Al<sub>2</sub>O<sub>3</sub>, 2.30 wt.% Na<sub>2</sub>O), P-140 olivine (7.41 wt.% FeO), Corning W glass (0.64 wt.% MnO) and Corning X glass (0.71 wt.% NiO). Analyses of low-Ca pyroxenes agree satisfactorily with those given by Howie and Smith (1963). Analyzed spots were noted on photographs for later ion-probe analysis because the pyroxene grains differed slightly in composition. In all, 7 olivine and 16 low-Ca pyroxene samples were selected for ion probe analysis in addition to many samples from peridotites. The preparation of the thin section and electron microprobe analyses added considerable surface contamination and a cleaning procedure was required before ion probe analysis. After final polishing with diamond compound, surfaces were cleaned with Q-tips and acetone followed by carbon tetrachloride and immediately coated with a conducting gold layer of  $\sim$ 25 $\text{Å}$  and stored in a dessicator. Gold is preferred over carbon because the Au layer can be sputtered faster, reduces the possibility of forming hydrocarbons during sputtering, and does not contribute to the SI spectrum.

#### Analytical conditions

Possibly the most difficult aspect in comparing ion probe results between different laboratories is the wide variety of instrumental conditions. Below are given our routine operating parameters with some justifications.

- (1) The primary beam is negatively charged oxygen which was shown (Andersen, 1969) to generally give high yield of positive SI for insulating samples. Primary beam intensities in excess of 100nA are routinely obtained from the duoplasmatron source. The beam is mass analyzed to provide a pure <sup>16</sup>O<sup>-</sup> beam by exclusion of species derived from the duoplasmatron itself, and from possible leaks, but at the expense of a reduced intensity.
- (2) The primary beam has an impact energy of 20kV; higher potentials might increase the sputtering and ion yields but are more susceptible to electrical breakdown.
- (3) The condenser lens is adjusted to give a 10nA primary beam current at a Faraday cup in the sample position from a maximum observed value of 90nA. This adjustment provides greater stability in the primary beam at the sample because the beam becomes insensitive to the various voltage fluctuations prior to the final aperture. Also by reducing the primary beam, the overall ion-optical properties allow better focusing of the primary beam to a routine diameter of  $\sim$ 15  $\mu$ m. The 10nA beam current was chosen to allow good SI intensities for a reasonably small spot. Because variations in primary beam intensity cannot be monitored during analysis, the current is measured before and after analysis by moving the sample from the beam path and collecting the beam in a Faraday cup. Observed drifts of primary intensity are less than 2% of the total over 20 minutes.
- (4) Although rastering of the primary beam in conjunction with an electronic aperture should provide a cleaner target surface without edge effects, we prefer to use a stationary focused beam. This gives a faster stabilization of the SI signal and does not consume as much material. Uncertainties or changes with time of edge effects in the periphery of the focused beam can be corrected by periodic reference to standards.
- (5) The sample is observed with both reflected and transmitted light. Special care in focusing with high power (150 $\times$ ) reflected light is necessary to ensure that the analysis point remains constant with respect to the SI extraction system.
- (6) Extraction of SI is provided by a number of focusing and deflecting electrodes between the sample and source slit of the mass spectrometer. The observed intensity ratios of SI and the position of the primary ion beam are greatly influenced by the potentials on these electrodes. As a set procedure all controls are adjusted to give maximum Si ion yield. The settings are nearly constant from day to day. Adjustments in the repeller and extractor potentials affect the position of the primary beam and are fixed during routine measurements. Deflection/centering ad-

Table 1. Compositions (wt.%) and secondary ion intensities for olivine

	*1	2	3	4	5	6	7
SiO <sub>2</sub>	41.3	38.8	36.8	35.5	30.8	29.7	29.6
FeO	7.4	19.0	30.7	38.3	60.7	65.9	67.6
MnO	0.10	0.25	0.39	0.56	1.10	0.97	2.30
MgO	50.9	41.9	32.5	26.4	6.43	2.51	0.08
NiO	0.33	0.12	0.06	0.01	0.00	0.00	0.00
CaO	0.004	0.19	0.04	0.03	0.16	0.06	0.10
TiO <sub>2</sub>	nd	0.029	0.014	nd	0.063	nd	0.010
Al <sub>2</sub> O <sub>3</sub>	nd	0.040	0.007	nd	0.008	0.007	nd
Na <sub>2</sub> O	nd	0.013	nd	nd	nd	nd	nd
Cr <sub>2</sub> O <sub>3</sub>	nd	0.014	nd	nd	nd	nd	nd
Σ	100.034	100.356	100.511	100.80	99.261	99.147	99.696

	Cations / 12 Oxygens						
Si	3.003	2.973	2.980	2.981	3.001	2.991	3.011
Fe	0.450	1.218	2.079	2.690	4.946	5.550	5.751
Mn	0.006	0.016	0.027	0.040	0.091	0.083	0.198
Mg	5.517	4.786	3.923	3.304	0.934	0.377	0.012
Ni	0.019	0.007	0.004	0.001	0.000	0.000	0.000
Ca	0.000	0.016	0.004	0.003	0.017	0.007	0.011
Ti	0.000	0.002	0.001	0.000	0.005	0.000	0.001
Al	0.000	0.004	0.001	0.000	0.001	0.001	0.000
Na	0.000	0.002	0.000	0.000	0.000	0.000	0.000
Cr	0.000	0.001	0.000	0.000	0.000	0.000	0.000
Mg/(Mg+Fe)	92	80	65	55	16	6	0.2

	Secondary ion intensity**						
Si	440	304	277	286	362	392	396
Fe	145	467	948	1160	2510	2990	3040
Mn	3.10	9.88	16.5	23.3	57.8	57.0	132
Mg	4320	4740	4230	3620	1020	434	13
Ni	1.56	1.06	0.69	0.15	0.10	0.01	nd
Ca	0.03	9.38	1.65	1.13	7.60	1.79	4.28
Co	0.26	0.51	1.10	0.99	0.62	0.28	0.01
Cr	1	110	nd	nd	nd	nd	nd
V	nd	2	1	nd	nd	nd	nd
Ti	8	260	60	4	710	50	77
Sc	3	4	7	3	18	10	3
Al	13	2170	400	55	700	40	78
K	8	9	5	13	22	15	13
Na	45	6100	121	106	265	118	105
Li	100	190	1120	2750	1080	1150	1660
P	2	5	7	13	13	6	3

\* Samples: 1. P-140 Balsam Gap N.C. dunite; 2. TS-4 = SCL1.3 (Simkin and Smith, 1970); 3. TS-8 = KI-2099 (Simkin and Smith, 1970); 4. TS-9 = YS-11 (Smith, 1966); 5. YS-5 (Smith, 1966); 6. TS-10 = L282 (Simkin and Smith, 1970); 7. R3517 = YS-1 (Smith, 1966).

\*\* Counts/sec x 10<sup>-3</sup> except for Cr, V, Ti, Sc, Al, K, Na, Li, P which are counts/sec. Count rates normalized to 100% isotopic abundance. Low mass resolution: Si, Fe, Mn, Mg Session 1. Mn, Co, Al, K, Na, Li, P Session 2 - normalized to Mn of Session 1. High mass resolution: Ni, Ca, Cr, V, Ti, Sc. nd - not detected.

justments just before the source slit are sensitive to the initial energy of the particular SI as well as to any misalignment of the extraction optics with respect to the analyzed point and source slit. These are changed for each measurement to give a maximum SI signal for each ion type.

(7) The source slit is adjustable from fully closed to 0.025 cm and, in conjunction with an adjustable collector slit, controls the mass resolution of the mass spectrometer. For low resolution, the collector slit is opened fully and the source slit adjusted to provide no more than about 10<sup>6</sup> cts/sec for the most intense peak to avoid damage to the first dynode of the electron multiplier and to avoid serious dead-time corrections. Under these conditions peaks have a top that is flat to ±1% of peak height. The extreme range in count rates between major and minor elements precludes collection of data under identical slit settings for both; however, some major elements, such as Si, have minor isotopes which can provide a SI signal of acceptable count rate with slits set for maximum sensitivity.

(8) Although the mass spectrometer allows photographic recording of SI spectra, exclusive use is made of electrical detection which incorporates a 20-stage electron multiplier, preamplifier and scaler with a 100 megaHertz counting capability.

(9) Magnetic peak switching at low mass resolution is automatic using an on-line Data General computer and an analytical relation between field intensity sensed by a Hall-effect probe and secondary magnet current. Peak switching over a 10 amu (atomic mass unit) range and stabilization of the magnetic field requires about 5 seconds. Because the present electronic configuration does not allow precise magnet scanning under high mass resolution, this is done manually with manual recording of data. Instrumental modification for scanning at high resolution is in progress, using the design developed at Cambridge, England (Long *et al.*, 1980).

(10) To allow for long-term drift and to provide an indication of precision, standard samples are analyzed at regular intervals. Such samples are chosen for homogeneity, grain size, and chemical proximity to the sample type being analyzed. A sequence of analyses is ignored if count rates on the standards change by more than 5%. These standards also allow comparisons from day to day for which the relative count rates may differ appreciably (±25%) even though analytical conditions are nominally identical.

Aside from the basic principle, important differences which are not always apparent exist between ion and electron probe techniques. (1) the SI spec-

Table 2. Compositions (wt.%) and secondary ion intensities for low-Ca pyroxenes

	*1	2	3	4	5	6	7	8	9	10	11	12	13	14	15	16
SiO <sub>2</sub>	56.8	57.8	54.7	55.7	55.8	53.5	52.4	53.5	51.2	52.8	49.9	50.6	50.7	49.0	49.1	47.3
TiO <sub>2</sub>	0.10	0.00	0.08	0.12	0.11	0.06	0.14	0.04	0.08	0.06	0.04	0.12	0.09	0.07	0.13	0.03
Al <sub>2</sub> O <sub>3</sub>	0.95	0.31	4.16	1.27	1.68	3.86	1.80	1.07	3.11	0.82	3.00	1.51	0.62	0.99	0.60	1.00
Cr <sub>2</sub> O <sub>3</sub>	0.38	0.12	0.08	0.50	0.16	0.22	0.00	0.01	0.00	0.00	0.03	0.01	0.00	0.00	0.00	0.00
FeO	4.40	6.60	10.0	10.7	13.1	14.4	22.0	24.1	24.2	24.7	28.0	29.9	31.0	34.8	36.2	41.5
MnO	0.09	0.09	0.28	0.23	0.24	0.30	0.62	0.73	0.76	0.87	0.57	0.53	1.02	0.66	0.90	0.91
MgO	35.0	35.2	31.6	30.6	30.0	27.8	23.2	22.9	21.2	21.6	18.6	17.8	16.3	13.7	12.6	8.8
NiO	0.11	0.07	0.06	0.07	0.02	0.09	0.00	0.01	0.01	0.01	0.01	0.01	0.00	0.01	0.00	0.00
CaO	0.47	0.07	0.43	1.20	0.46	0.66	0.63	0.29	0.30	0.60	0.29	0.80	0.72	0.50	0.93	0.91
Na <sub>2</sub> O	0.15	0.00	0.00	0.01	0.00	0.01	0.01	0.00	0.02	0.02	0.00	0.01	0.01	0.01	0.02	0.01
Σ	98.45	100.26	101.39	100.40	101.57	100.90	100.80	102.65	100.88	101.48	100.44	101.29	100.46	99.74	100.48	100.46
<b>Cations / 12 Oxygens</b>																
Si	3.950	3.975	3.790	3.920	3.909	3.806	3.876	3.910	3.820	3.926	3.811	3.869	3.938	3.907	3.921	3.888
Ti	0.005	0.0	0.004	0.006	0.006	0.003	0.008	0.002	0.004	0.003	0.002	0.007	0.006	0.004	0.008	0.002
Al	0.078	0.025	0.340	0.105	0.139	0.324	0.157	0.092	0.274	0.072	0.270	0.136	0.057	0.093	0.057	0.097
Cr	0.021	0.006	0.004	0.028	0.009	0.012	0.000	0.001	0.000	0.000	0.002	0.001	0.000	0.000	0.000	0.000
Fe	0.256	0.380	0.580	0.630	0.767	0.857	1.360	1.473	1.510	1.536	1.788	1.912	2.014	2.321	2.418	2.853
Mn	0.005	0.005	0.016	0.014	0.014	0.018	0.039	0.045	0.048	0.055	0.037	0.034	0.067	0.045	0.061	0.064
Mg	3.628	3.608	3.264	3.210	3.132	2.948	2.556	2.495	2.357	2.394	2.117	2.029	1.887	1.628	1.500	1.078
Ni	0.006	0.004	0.003	0.004	0.001	0.005	0.000	0.001	0.001	0.001	0.001	0.001	0.000	0.001	0.000	0.000
Ca	0.035	0.005	0.032	0.090	0.034	0.050	0.050	0.023	0.024	0.048	0.024	0.066	0.060	0.043	0.080	0.080
Na	0.020	0.000	0.000	0.001	0.000	0.001	0.001	0.000	0.003	0.003	0.000	0.002	0.002	0.002	0.003	0.002
En	92.6	90.4	84.2	81.7	79.6	76.5	64.5	62.5	60.6	60.2	53.9	50.6	47.6	40.8	37.5	26.9
Fs	6.6	9.5	15.0	16.0	19.5	22.2	34.2	36.9	38.8	38.6	45.5	47.7	50.8	58.1	60.5	71.1
<b>Secondary ion intensity**</b>																
Si	285	314	285	291	312	274	240	274	238	252	246	246	255	247	262	267
Ti	990	120	1010	1560	880	570	1570	550	850	950	450	1050	920	960	1380	280
Al	24.3	9.62	108	41.0	59.2	129	61.7	33.1	107	31.6	109	40.7	18.5	32.5	20.5	38.4
Cr	3650	990	750	5800	1880	2330	2	240	25	25	320	78	8	56	7	nd
Fe	59	84	124	159	210	215	328	376	380	404	447	472	519	545	605	684
Mn	1.80	1.77	6.1	5.13	6.1	6.81	13.2	17.4	15.5	20.6	13.5	13.5	23.6	15.2	22.2	24.0
Mg	1550	1530	1350	1530	1610	1390	1160	1270	1050	1160	1000	918	873	709	709	518
Ni	725	387	187	404	104	544	211	126	98	23	66	88	38	109	41	50
Ca	1.55	0.27	1.15	5.01	1.56	1.97	2.52	1.28	1.08	2.05	0.93	1.94	2.84	1.67	3.42	2.15
Na	33.2	0.48	0.26	7.39	2.00	2.93	2.04	0.99	1.62	2.40	1.55	3.82	2.15	0.82	2.91	2.01
Co	28	39	46	80	68	100	108	130	119	79	108	122	129	176	92	17
V	58	39	99	170	120	71	43	97	100	15	170	67	30	110	21	nd
Sc	6	16	44	89	68	40	78	86	170	53	61	48	160	90	180	34
K	240	960	410	6100	580	430	450	1200	250	340	440	38000	260	400	310	580
Li	740	2900	6800	1200	7200	5800	1300	3900	9900	2600	7900	1400	4600	2200	6400	470
P	13	12	22	7	18	21	6	9	16	5	10	22	4	4	6	4

\*Samples: 1. 73-165; 2. SAG; 3. R62; 4. Y18; 5. E21; 6. H66; 7. Y9; 8. R13b; 9. SP18; 10. Z2270; 11. 2941; 12. 7286; 13. 137; 14. 4642A; 15. 115; 16. 1002.

\*\*Counts/sec  $\times 10^{-4}$  except for K, Ti, Cr, Ni, Co, V, Sc which are counts/sec. All count rates normalized to 100% isotopic abundance.

Low mass resolution: Si, Al, Fe, Mn, Mg, Na, K, Li, P from one analysis session. High mass resolution: Ti, Cr, Ni, Ca, Co, V, Sc from second analysis session.

nd: not detected

trum contains no equivalent of the intense white radiation background which statistically limits precision with the electron probe. Ion probe precision is only limited by instrument stability and peak count-

ing statistics. (2) Whereas the ratio of X-ray intensity to concentration varies little for different elements with  $11 < Z < 26$ , SI signals range over 5 orders of magnitude resulting in a wide range of sensitivities

for different elements. (3) An X-ray signal stabilizes quickly after the electron beam impinges on the sample, whereas the ion beam requires ~5 minutes to produce a stable SI signal. Thus points cannot be analyzed at a rate comparable to that possible with the electron probe. Rastering of the primary beam requires considerable time to give a stable SI signal from a large area, whereas imaging with an electron probe is rapid. (4) Sample change requires several hours for the ion probe in order to maintain a clean vacuum of  $10^{-8}$  torr.

In practice, approximately 30 mineral analyses for ~10 elements are possible in a 10 hour day. Because many elements can be analyzed under low mass resolution, whereas others require high mass resolution to separate interferences, two sessions are required to obtain a complete analysis; reproducible, rapid switching from low to high mass resolution is not feasible.

#### Mass spectrum of Mg,Fe silicates

The first step in analysis of a mineral matrix is an examination of the SI mass spectrum. As a guide to possible interferences a computer-generated list is first made for a specific set of matrix elements. For olivine and low-Ca pyroxene a matrix was prepared for Mg, Fe, Si, Al, Ca and O. Although the most abundant isotope is the obvious choice for analysis, it might be preferable to collect intensity data at low mass resolution for a weaker isotope if the attenuation of transmission of the abundant isotope at high mass resolution reverses the advantage in sensitivity. The absence of an interference for a weaker isotope is more difficult to confirm at high mass resolution because the transmission is lower, and a wide range of compositions must be examined so that an interference is not overlooked when it occurs only in some specimens.

These particular problems are illustrated by mass scans for the five Ti isotopes in an olivine (Fig. 1). From the known isotopic ratios for  $m/e$  (= charge to mass ratio) of 46–50 (8.0, 7.8, 73.4, 5.5, 5.3%), large interferences at 46, 48, 49, and 50 must have raised the intensity relative to that of 47. From the computer-generated list of mass defects (Table 3), most interferences can be assigned easily: e.g.,  $^{24}\text{Mg}_2^+$  at  $m/e = 48$ . Although  $m/e = 47$  appeared to be interference-free from both the absence of computer-generated interferences and high-resolution scans, intensity data obtained at high resolution for  $m/e = 48$  and low resolution for  $m/e = 47$  for a range of olivines did not fall on a single line passing through

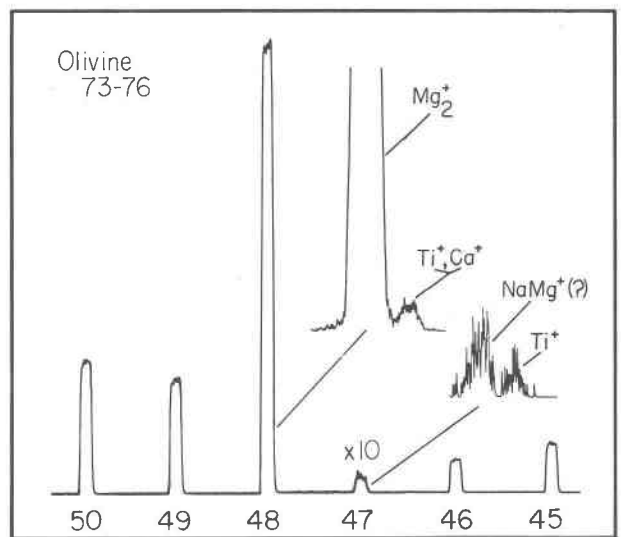


Fig. 1. Low resolution mass scan of titanium isotopes in 73–76 olivine (Fo 94,  $\text{TiO}_2 \approx 30$  ppm,  $\text{Na}_2\text{O} = 120$  ppm) from garnet lherzolite. Isotopes at  $m/e = 50, 49, 48,$  and  $46$  clearly have large interferences because  $m/e = 47$  is very weak. Insets show high mass resolution scans illustrating that even  $m/e = 47$  has an interference thought to be  $\text{NaMg}^+$ .

zero (Fig. 2). The simplest explanation was that some samples have an interference at  $m/e = 47$ , and indeed high-resolution scans on samples with excess counts at  $m/e = 47$  on Figure 2 showed a doublet (Fig. 1). The only plausible interference was  $^{23}\text{Na}^{24}\text{Mg}^+$  and indeed the Na content of olivine correlates qualitatively with the excess low-resolution signal at  $m/e = 47$  on Figure 2, as indicated by the dashed line for samples with  $\text{Na} > 25$  ppm. This interference could have been overlooked quite easily because Na is absent at the 40 ppm ( $2\sigma$ ) detection level of the electron microprobe in most olivines crystallized at low pressure ( $< \sim 10$  kbar), and only olivines from the deep-seated peridotites display Na substitution consistently. The  $^{23}\text{Na}^{24}\text{Mg}^+$  interference is significant because of the very high yield of secondary ions involving alkali metals. Titanium analyses must be obtained at high mass resolution for Na-bearing olivines. For Na-free olivines, low resolution analysis at  $m/e = 47$  gives a higher sensitivity than high resolution at  $m/e = 48$ .

Whether the analytical technique uses high mass resolution or energy filtering to suppress interferences, it is necessary to first identify the magnitude of the interference. Table 4 summarizes the systematic examination of interesting elements represented in the spectra of (Mg,Fe) silicates. Undoubtedly other elements can be detected. Some general features are: (1) for elements with  $Z < 12$ , interferences

Table 3. Interferences for Ti isotopes from mafic silicate

m/e	species	mass defect (milli mass units)	resolution (M/ $\Delta$ m)
46	Ti	-47.4	-
	<sup>30</sup> SiO	-31.3	2860
47	Ti	-48.2	-
48	Ti	-52.1	-
	Ca	-47.6	10700
	<sup>24</sup> Mg <sub>2</sub>	-30.0	2170
49	Ti	-52.1	-
	<sup>24</sup> Mg <sup>25</sup> Mg	-29.2	2140
50	Ti	-55.2	-
	<sup>24</sup> Mg <sup>26</sup> Mg	-32.4	2330
	<sup>25</sup> Mg <sub>2</sub>	-28.4	1960

can result only from multiply charged species. Possible interferences at  $m/e = 6$  and  $7$  for  $Mg^{+4}$  and  $Si^{+4}$ , respectively, are not detectable, and H, Li, B, F and Na can be measured at low mass resolution. (2) For elements between  $Z = 20$  and  $Z = 30$  (Ca–Zn), molecular interferences, usually singly-charged oxides or metal dimers, are intense for the major isotopes. In Table 4, the interference intensity, expressed as cts/sec, can be used to approximately calculate ratios of interference to analytical peaks. For example, 500 ppm Ca would give an intensity of approximately 3750 cts/sec ( $500 \times 6.5$  cts/sec) while the MgO interference would give  $\sim 1500$ – $5000$  cts/sec for a ratio between 1:4 and 1:1.3.

### Major-element systematics

The variation of major-element SI signals with composition should provide tests of postulated correction procedures and theories of interactions which occur during sputtering and ionization. Although the same information can be obtained from minor elements, major-element data are much easier to use because of high count rates, negligible interferences and well-known composition either from stoichiometry or electron-probe analysis.

The simplest presentation is a plot of raw count rate against the atomic concentration as in Figure 3a, b where  $Mg^+$ ,  $Fe^+$  and  $Si^+$  are plotted against mole% forsterite or enstatite ( $mg = Mg/(Mg + Fe)$ ) for olivine and pyroxene, respectively. Although the atomic fraction of silicon is near-constant for all olivines, the SI yield changes drastically with a minimum near  $mg = 0.65$  and a greater yield for the Mg than for the Fe end member. Whereas Fe count rates show a mono-

tonic but non-linear decrease from Fe-rich to Fe-poor compositions, for Mg there is a maximum SI yield near  $mg = 0.8$  and a decrease in intensity for higher  $mg$ . A second set of nearly identical data for these same samples was given by Steele and Hutcheon (1979). Data for low-Ca pyroxenes (Fig. 3b) are more difficult to interpret because of higher levels of minor elements and substitution of Al for Si. However, if the SI count rate for Si is normalized to the Si content from electron probe determination, the simple plot of normalized count rates vs. Si content shows considerable scatter but with a minimum value near  $mg = 0.60$  as for olivine. Iron shows an apparent linear relation with Fe atomic content. In contrast to olivine, Mg SI intensities do not show a clear maximum, but show considerable scatter about a line.

These variations of Mg, Si and Fe intensities clearly indicate the presence of complex interactions which affect the SI yields. Two important implications for any data reduction procedure are: (1) normalization of intensities to the SI count rate for silicon (Shimizu, 1978; Shimizu *et al.*, 1978) will introduce a systematic deviation from linearity unless both intensities show identical compositional dependence. For some compositional systems (Shimizu *et al.*, 1978), linear plots of atomic ratio ( $N_M/N_{Si}$ ) vs. intensity ratio ( $I_M/I_{Si}$ ) were found. However the data in Figures 3a and 3b do not give linear plots, and the

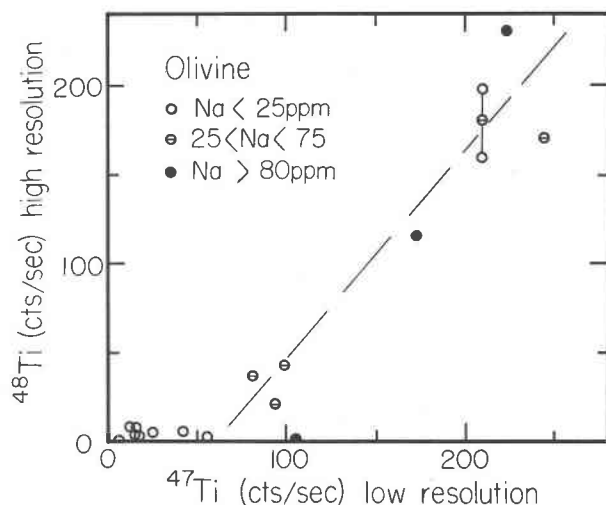


Fig. 2. Comparison of secondary ion count rates for  $^{48}Ti$  at high resolution and  $m/e = 47$  at low resolution for a suite of olivines from peridotites ranging from  $Fo_{88}$  to  $Fo_{94}$ . The dashed line was fitted by eye between the data for samples with  $Na < 25$  ppm. Because it does not pass through the origin, an interference is implied at  $m/e = 47$ .

compositional dependence of  $I_M/I_{Si}$  is affected by the complex form of the Si yield vs. composition curve. Although the Fe SI data appear near-linear with the atom fraction of Fe for both olivines and low-Ca pyroxenes,  $I_{Fe}/I_{Si}$  would be distinctly non-linear. (2) Use of "relative sensitivity factor" data for derivation of atomic ratios (Meyer, 1978; Storms *et al.*, 1977) has severe limitations because of compositional dependence. For the data of Figure 3a, the sensitivity factor of Mg in olivine ranges (Fig. 4) from about 3 for forsterite to 11 at Fo 60; for Fe, the sensitivity factor ranges from 8 to 4. Data in Meyer (1978) show at least 2-fold variations for Li, Be, F, Fe, Zr and Rb, depending on the standard. Although such diagrams are useful for illustration of wide sensitivity ranges, errors in deriving atomic ratios therefrom are large.

A simple relation is obtained between the observed  $Mg^+/(Mg^+ + Fe^+)$  SI ratio and the  $Mg/(Mg + Fe)$  atomic ratio (Fig. 5, center), but not for the corresponding  $Mg/(Mg + Si)$  plot (Fig. 5, upper left). Smooth trends occur for the  $Mg/(Mg + Fe)$  plot, but with slightly different trends for olivine and low-Ca pyroxene. Three reference curves with  $K = 1.0, 0.6$  and  $0.4$  are drawn for the following analytical form:

$$K = [mg(1 - mg^+)]/[(1 - mg)mg^+]$$

where  $mg = \text{atomic Mg}/(\text{Mg} + \text{Fe})$  and  $mg^+ = \text{SI ratio } Mg^+/(Mg^+ + Fe^+)$ . The data for low-Ca pyroxene (squares) lie close to a curve with  $K = 0.52$ , and the scatter of about  $\pm 1$  atomic % in  $mg$  is comparable to that for routine electron microprobe analyses. The data for six olivines have stayed consistent during several tests over two years, and yield  $K = 0.42$ . A larger suite of olivines with specimens of intermediate  $mg$  is needed to provide a more rigorous test. The advantage of using Figure 5 for  $mg$  determination is that only one standard is needed to confirm the value of  $K$ , and the analytical function is easy to handle.

The shape of the reference curves in Figure 5 indicates a constant distribution between Mg and Fe secondary ions to Mg and Fe atoms in the target, and is the same as that used for ideal solution models of site populations (*e.g.*, Saxena, 1973). Perhaps this regularity results from the similarity of chemical properties of  $Mg^{2+}$  and  $Fe^{2+}$  ions, and can be exploited in the theory of sputtering.

#### Minor and trace elements

In order to evaluate the experimental accuracy and the matrix influence, analyses of minor and trace ele-

ments by electron and ion microprobes are now compared. Although every effort was made to analyze identical areas with the two techniques, it must be emphasized that the ion probe uses SI sputtered from the surface whereas the electron probe uses X-rays excited from a light-bulb-shaped region with mean depth about 1 to 2  $\mu\text{m}$  below the surface. Tiny inclusions and exsolution lamellae, especially of Ca-rich pyroxene, are particularly troublesome in low-Ca pyroxene, and the pyroxene specimens represented in the figures are separated into groups for which electron probe analyses showed variable or near-constant analyses of Ca (Howie and Smith, 1966). Data from Tables 1 and 2 are now shown graphically and discussed.

#### Ca

Figures 6a and 6b compare ion and electron microprobe analyses for low-Ca pyroxene and olivine, respectively. If the inhomogeneous samples 4, 12 and 16 are ignored, there is a linear correlation within  $\pm 10\%$  absolute of the electron-probe values (dashed lines), especially for samples with constant Ca (square symbols). Furthermore there is no systematic bias with Mg/Fe about the visually-drawn central lines. The Ca level in olivine is much lower than in pyroxene, and multiple analyses were made with a narrow electron beam in the electron probe to test sample homogeneity in the area analyzed with the ion probe (Fig. 6b). Analyses were also made on the same spots on two separate days (open and filled circles). Samples 5 and 6 yielded a range in electron probe analyses considerably greater than the statistical error of the electron probe. There is considerable scatter about the visually-fitted linear averages and deviations tend to be the same for the two days, as particularly displayed by specimens 2 and 6 which have the largest deviations. Because Mg-rich specimens 2 and 3 lie above the lines and Mg-poor specimens 6 and 7 (marginally) lie below the lines, while specimens 4 and 5 are near the line, it appears that the SI yield for Ca may be higher for Mg-rich than Mg-poor olivines. Such a matrix effect must be confirmed by measurement of more specimens before it can be justified. A scatter of similar size was found for Mg determinations in plagioclase (Steele *et al.*, 1977b), but absence of a correlation with Na/Ca ratio indicated that there was no matrix effect. These two studies indicate the need for caution in assuming a linear dependence for ion probe analyses of minor elements in a mineral group with large compositional

Table 4. Analytical details for elements in Mg, Fe silicates

Isotope	% Abundance	Possible Interference <sup>a</sup>	$\Delta m(\text{mmu})$	RP(W/ $\Delta m$ )	cts/sec/ppm <sup>b</sup>	Comments
<sup>1</sup> H	100	-	-	-	? (L)	Problem with background H contamination. Background counts reduced to ~20/sec after several days at 10 <sup>-8</sup> torr. Clean vacuum essential for H analysis.
<sup>6</sup> Li	7.4	<sup>24</sup> Mg <sup>+4</sup>	-13.4	550	-	Neither Mg <sup>+4</sup> or Si <sup>+4</sup> interference has been observed. Lithium isotope ratios are feasible although accuracy of ion probe may not be sufficient for natural variations. Small scattered ion background at m/e = 7.
<sup>7</sup> Li	92.6	<sup>28</sup> Si <sup>+4</sup>	-18.9	320	~600(L)	
<sup>9</sup> Be	100	<sup>27</sup> Al <sup>+3</sup>	-18.4	490	-	Be thus far not detected in terrestrial olivine and low-Ca pyroxene. Al <sup>+3</sup> interference definitely present. Small scattered ion background.
<sup>11</sup> B	81	-	-	-	-	B thus far not detected in terrestrial olivine and low-Ca pyroxene. Some background due to scattered ions. Detection level should be ~100 ppb.
<sup>19</sup> F	100	-	-	-	? (L)	Intensity at m/e = 19 definitely varies from sample to sample suggesting F is present rather than contaminant. Absolute level is uncertain due to lack of standards.
<sup>23</sup> Na	100	<sup>30</sup> Si <sup>16,+2</sup> <sup>0</sup> P	-5.4	4260	~100(L)	Na contamination is major problem unless samples are carefully cleaned. SiO interference can be monitored at m/e = 22.5 at low resolution and is less than 0.5% of Na count rate for Na concentrations in olivine.
<sup>27</sup> Al	100	<sup>54</sup> Fe <sup>+2</sup> <sup>26</sup> Mg <sup>+2</sup> <sup>26</sup> NiH	-11.7 -0.4 -8.9	2310 68000 3030	~15(L)	Fe and MgSi interferences insignificant based on scans of m/e = 28.5 and 26.5, respectively. MgH is eliminated by cooling extraction optics with liquid N <sub>2</sub> .
<sup>31</sup> P	100	<sup>30</sup> Si <sup>10,+2</sup> <sup>30</sup> SiH	8.0 7.8	3880 3230	~0.5(L)	<sup>29</sup> Si <sup>10,+2</sup> is observed at m/e = 30.5 but SiH is eliminated by cooling extraction optics with liquid N <sub>2</sub> . Correction must be made for <sup>29</sup> Si <sup>10,+2</sup> based on 30.5
<sup>39</sup> K	93.1	<sup>23</sup> NaO <sup>24</sup> Mg <sup>54,+2</sup> <sup>Fe</sup> 0,P	+21.0 -1.4	1860 28000	~400(?) (L)	MgFe is not observed at m/e = 40.5 but NaO is present even for very low Na levels. Contamination of K is a definite problem and careful sample cleaning is required. Absolute levels uncertain due to lack of standards.
<sup>40</sup> Ca	97.0	<sup>24</sup> MgO <sup>24</sup> Mg <sup>Fe+2</sup>	27.8 -2.6	1440 15400	~ 6.5(H) ~ 15000-5000	Intense MgO interference. MgFe presence cannot be confirmed but is low based on absence of peak at 40.5 and general absence of doubly charged species.
<sup>45</sup> Sc	100	<sup>29</sup> SiO	15.5	2900	~2 (H) ~200-100	Sc has been detected in nearly all olivines and low-Ca pyroxenes.
<sup>47</sup> Ti	7.3	<sup>23</sup> Na <sup>24</sup> Mg <sup>Fe</sup> P,0	23.0	2045	~0.2 (H) ~50.2	NaMg interference is significant for this minor Ti isotope. Identification confirmed by correlation with Na content of low-Ca pyroxene.

Table 4. (continued)

<sup>48</sup> Ti	73.9	48Ca	P, O	4.5	10700	(H)	Ca interference cannot be resolved; Ca intensity at m/e = 48 is 0.00186 of Ca intensity at m/e = 40 and is generally trivial for olivine and low-Ca pyroxene
		24Mg <sub>2</sub>	O, P	24.4	2100	~2000-10	
<sup>51</sup> V	99.8	25Mg <sup>26</sup> Mg	O, P	24.4	2100	(H)	Mg <sub>2</sub> and MgAl interference intense relative to V content of Mg-rich natural samples.
		24Mg <sup>27</sup> Al	P	22.5	2270	~30-0	
<sup>52</sup> Cr	83.8	24Mg <sup>28</sup> Si	O, P	21.4	2430	(H)	
		26Mg <sup>27</sup> Al	O, P	24.7	2110	~2400-20	Combination of interferences gives high Int/Pk ratio.
<sup>55</sup> Mn	100	25Mg <sup>27</sup> Al	P	26.8	1940	(L)	FeH is eliminated by cooling extraction optics with liquid N <sub>2</sub> . MgSi is generally minor relative to Mn levels in natural samples.
		54FeH	O, P	9.3	5900	~40-0	
<sup>59</sup> Co	100	30Si <sup>29</sup> Si	O, P	17.1	3340	~20(L)~0.3(H)	FeH is eliminated by cooling extraction optics with liquid N <sub>2</sub> . CaO and AlO <sub>2</sub> interferences are significant in pyroxene but not in olivine. Si <sub>2</sub> is not observed. Pyroxene thus requires high resolution.
		43Ca <sup>16</sup> O	P	20.5	2870	~5	
<sup>60</sup> Ni	26.2	27Al <sup>16</sup> O <sub>2</sub>	P	38.1	1550		
		58FeH	O, P	7.9	7550		
<sup>63</sup> Cu	69.1	28Si <sup>16</sup> O	O, P	35	1670	(H)	Fe at m/e = 58 precludes using <sup>58</sup> Ni. Si <sub>2</sub> interference is not seen for olivine but is definitely present for low-Ca pyroxene.
		30Si <sub>2</sub>	P	16.8	3570	~50-0	
<sup>66</sup> Zn	27.8	40Ca <sup>23</sup> Na	P	22.8	2760	?	Cu not observed in natural samples. Interference mainly due to TiO.
		24Mg <sup>23</sup> NaO	P, O	40.1	1470		
		47TiO	P, O	17.1	3680		
		Mg <sub>2</sub> O	O, P	~36	1810	(H)	Zn has not been detected in natural olivines and low-Ca pyroxenes. All interferences are present as determined by scans on a variety of samples.
		27Al <sup>23</sup> NaO	P	40.2	1640		
		MgCa	O, P	~19.2	3400		
		50TiO	O, P	13.7	4820		
		50CrO	O, P	15.0	4400		

<sup>a</sup>O, P refer to presence in olivine or low-Ca pyroxene, respectively.

<sup>b</sup>Observed counts/second/ppm at 10nA for analytical peak at low (L) or high (H) resolution as required. Also given are count rates (cts/second) for the interfering peak. Two entries represent interference level in Mg- or Fe-rich compositions.

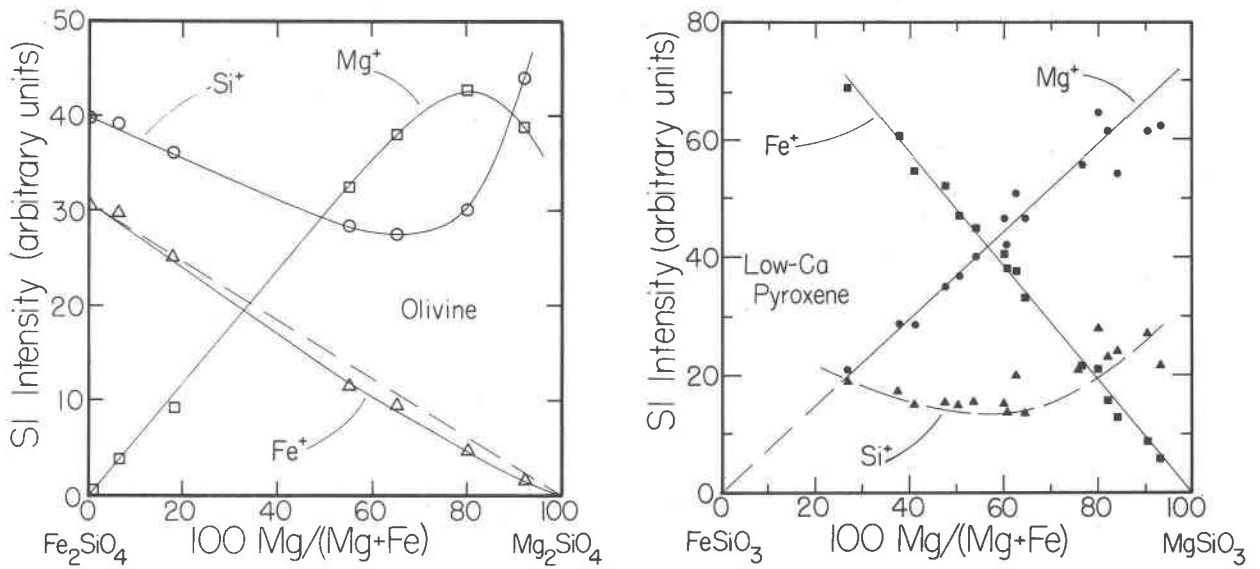


Fig. 3(a) Variation of secondary ion count rates for  $Si^+$ ,  $Mg^+$  and  $Fe^+$  in olivine as a function of forsterite content. (b) Variation of secondary ion count rates for  $Si^+$ ,  $Mg^+$  and  $Fe^+$  in low-Ca pyroxene as a function of enstatite content. Curves for  $Mg^+$  and  $Fe^+$  are possibly linear while  $Si^+$  is not. Lines fitted by eye.

variation of major elements. For a CAMECA ion microprobe, Shimizu *et al.* (1978) found that the Ca yield for ferromagnesian minerals was enhanced in Fe-rich samples. Detailed measurements of the same samples with CAMECA and AEI ion microprobes are needed to test whether the apparent difference in matrix effects results from instrumental parameters (*e.g.*, degree of energy selection of the secondary ions) or from choice of normalization (Shimizu *et al.* normalized SI intensities to those of Si).

Figure 7 demonstrates that there is a nearly linear correlation between electron and ion probe analyses of Ca in olivines for which the range of *mg* is small enough (0.85–0.94) for matrix effects to be low. All the samples are from peridotite nodules in kimberlites. The electron microprobe analyses were obtained on thin sections whereas the ion probe analyses were made on grain mounts. Much of the scatter lies within the  $2\sigma$  counting precision of the electron probe analyses, and a small amount can be ascribed to mineral inhomogeneity detected in the electron probe analyses. Even if all the scatter were attributed to the ion probe (for which the counting precision is trivial), most analyses would lie within a  $\pm 10\%$  range.

Data taken in one analytical session (Fig. 8) demonstrate that the SI yield for low-Ca pyroxenes is about one-third higher than for olivines, as also was found for Mn (see below).

#### Ni

A less favorable peak/background ratio for the electron probe, lower concentrations of Ni, and positive correlation of Ni and Mg in natural samples make comparisons of Ni determinations more difficult than for Ca. Because ion and electron probe analyses of Ni in low-Ca pyroxene (Table 2; filled circles, Fig. 9a) correlated poorly, repeat determinations were made with both the electron probe and ion probe (open circles) for four out of the five samples showing highest Ni. The relative position of each

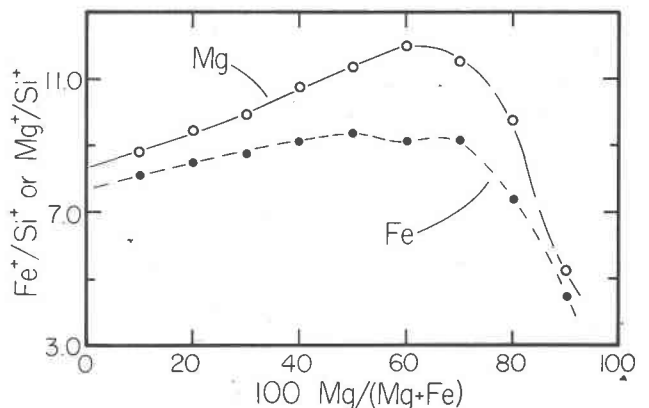


Fig. 4. Variation of Mg and Fe secondary ion "sensitivity factor" ( $= Mg^+/Si^+$  or  $Fe^+/Si^+$ ) for olivine as a function of forsterite content.

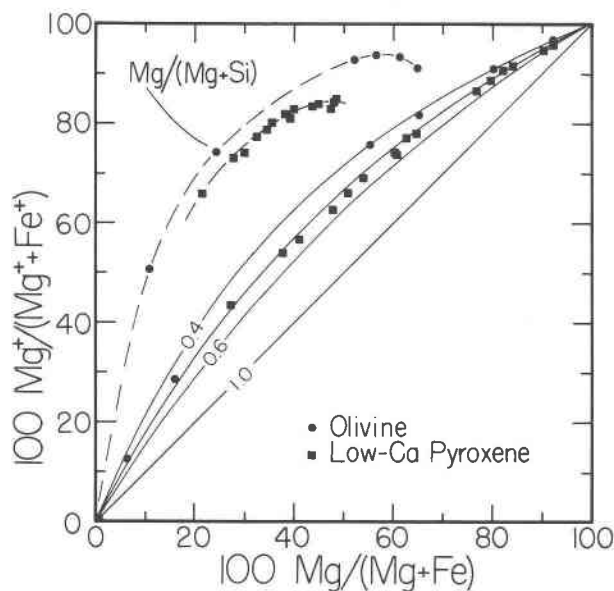


Fig. 5. Variation of  $mg$  ( $= 100 \text{ Mg}/(\text{Mg} + \text{Fe})$  atomic) in target with secondary ion  $mg^+$  ( $= 100 \text{ Mg}^+/(\text{Mg}^+ + \text{Fe}^+)$ ) for olivine and low-Ca pyroxene. Dashed lines show variation of  $100 \text{ Mg}/(\text{Mg} + \text{Si})$  in target as a function  $100 \text{ Mg}^+/(\text{Mg}^+ + \text{Si}^+)$  of secondary ion spectra. See text for discussion.

point is qualitatively the same for the two determinations although the ion probe count rate is about 40% lower for the second determination. The scatter about any correlation line is large even if analytical errors or zoning are considered. Following the observation by Reed *et al.* (1979) that the Ni yield is a function of the Fe content of olivine, we tested the effect of the Fe/Mg ratio of low-Ca pyroxene on the Ni SI yield. Figure 10a shows a near-linear correlation between the Fe content expressed as mole% ferrosilite and the Ni yield ( $\epsilon$ ):

$$\epsilon = (\text{atomic Fe/Ni}) \cdot (\text{ion probe cts Ni/Fe})$$

If the Ni SI yield were independent of the Fe/Mg ratio, the points on Figure 10a would lie on a horizontal line. The positive slope indicates that with increasing Fe (thus decreasing Mg), the same atomic concentration of Ni gives greater Ni SI yield.

Similar data are given on Figures 9b and 10b for the four olivines for which Ni is detectable with the electron probe. Again, an approximate linear dependence of  $\epsilon$  with Fe expressed as mole% fayalite is present. Comparison with the results of Reed *et al.* (1979) is complicated because Reed *et al.* obtained both the Ni and Fe analyses at high resolution whereas the present data for Fe were taken at low resolution. Furthermore the extraction optical system in the AEI ion microprobe used by Reed *et al.* is not

the same as that at Chicago, and a different energy band of the SI may be used. It appears from the difference of slopes of lines in Figure 10b that an empirical matrix correction must be determined for each set of analytical conditions. In view of the non-linearity of data in Figure 3a, it is possible that the trends in Figures 10a and 10b would be found to be slightly non-linear if further measurements of higher precision were made.

### Mn

This element shows a strong correlation with Fe, as shown by the progression of sample numbers along the band of data in Figures 11a and 11b for low-Ca pyroxene and olivine. Because the data points are randomly scattered about a straight line, there is no evidence for a change of ionization efficiency with Fe/Mg ratio, as was demonstrated for Ni. However Figure 12 shows that the SI yield for Mn in low-Ca pyroxene is about 25% greater than for olivine. It should not be assumed that this difference of "relative sensitivity factor" is constant from one ion microprobe to another and from one set of operating conditions to another.

### Al

There is a good linear correlation (Figure 13) for the four low-Ca pyroxenes (squares) listed as homogeneous by Howie and Smith (1966), and all but two of the inhomogeneous specimens (filled circles) lie close to the line. There is no evidence for a matrix effect dependent on the Fe/Mg ratio.

Because the Al content of olivine is rarely much greater than the detection level with the electron microprobe (70 ppm  $\text{Al}_2\text{O}_3$  at  $2\sigma$ ), it was not possible to make a rigorous calibration of ion probe analysis. However, all olivines with Al detected with the electron microprobe show high count rates with the ion probe.

### Cr

Because of the rapid decrease of Cr with increase of Fe in low-Ca pyroxene, only a few samples could be used to test ion probe analysis. For these samples, there is a linear relation (Fig. 14) between electron and ion probe analyses, with the scatter mostly within the  $2\sigma$  counting error of the electron microprobe analyses. Only one olivine contained Cr at the detection level of the electron microprobe, and it had a substantial ion probe signal. Chromium occurs at detectable levels in olivines from deep-seated peridotites, and there is a good correlation between electron

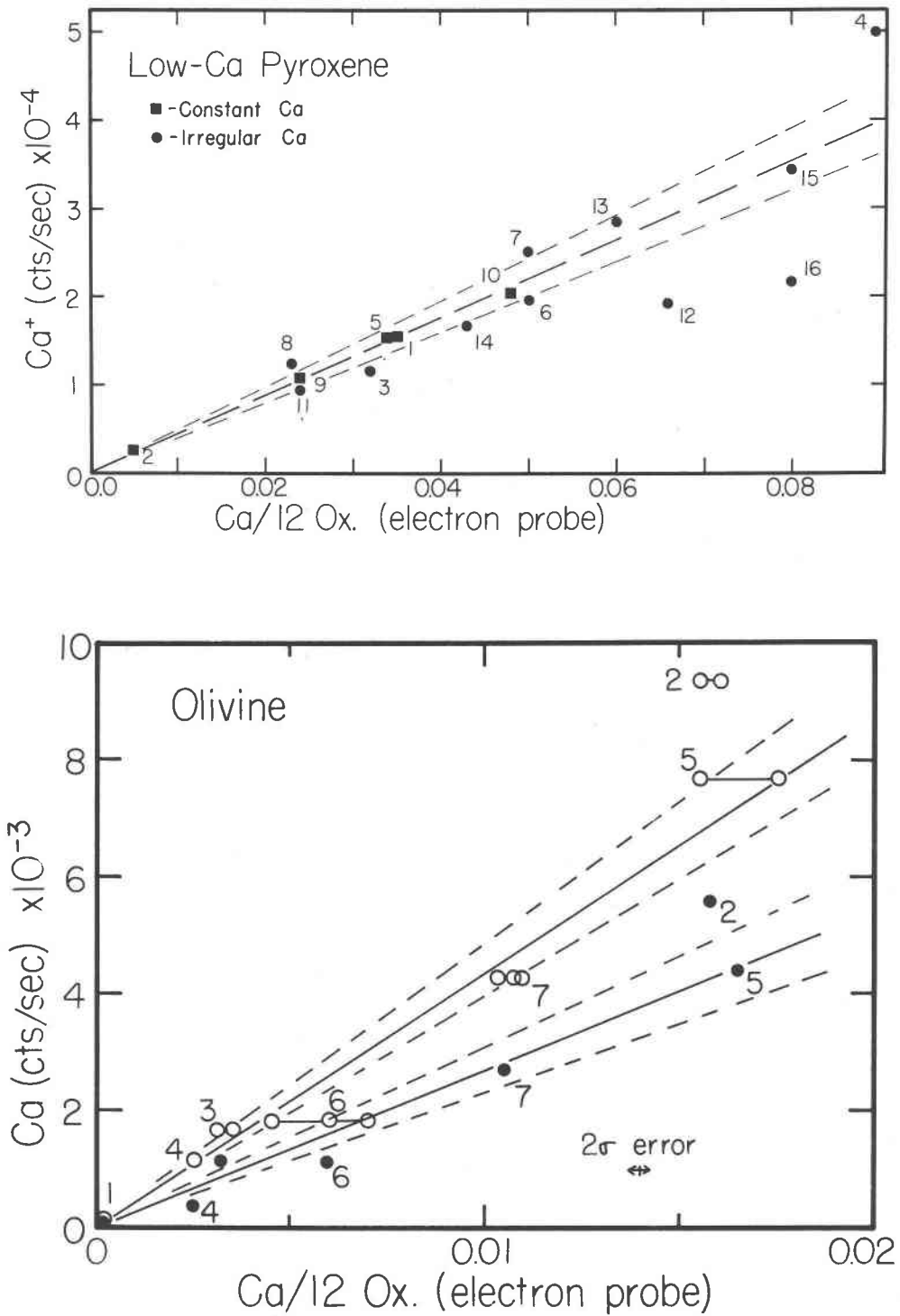


Fig. 6(a)  $\text{Ca}^+$  secondary ion count rate vs. Ca cations /12 oxygens in low-Ca pyroxene. Numbers adjacent to data points correspond to analyses in Table 2 and higher sample numbers represent samples richer in Fe. Square symbols are used for samples known to have constant Ca and circles for those with variable Ca. Dashed lines represent  $\pm 10\%$  absolute errors from eye-estimated linear fit. (b)  $\text{Ca}^+$  secondary ion count rate vs. Ca cations/12 oxygens in olivine. Open and solid symbols represent analyses made on different days. Dashed lines represent  $\pm 10\%$  absolute errors from eye-estimated linear fit. Sample numbers are shown.

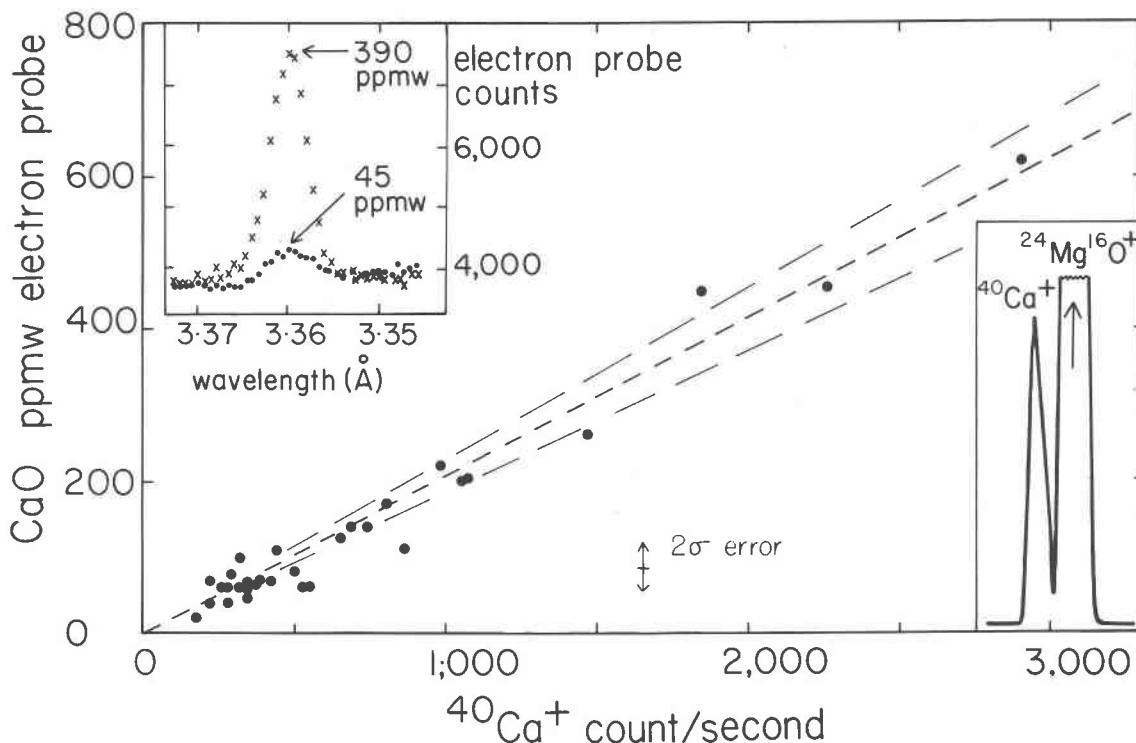


Fig. 7. Ca<sup>+</sup> secondary ion count rate vs. Ca ppm for olivines from peridotites. At these low concentrations, mole fraction is proportional to weight fraction. Upper left inset shows electron probe wavelength scans for 390 and 45 ppmw CaO and lower right inset shows ion probe mass scan at high resolution to separate MgO<sup>+</sup> molecular interference from <sup>40</sup>Ca<sup>+</sup>. Error is based on counting statistics.

and ion probe analyses; however, the small range of Fe/Mg in these samples precludes testing for a matrix effect.

*Ti*

The ion probe signal at <sup>48</sup>Ti has an unresolved <sup>48</sup>Ca interference even at high resolution, but the interference is small for low-Ca pyroxene (Fig. 15: circle, uncorrected; dot, corrected) and trivial for olivine. The correction was made by dividing the count rate for <sup>40</sup>Ca by the accepted isotopic ratio of 97.0:0.18 for <sup>40</sup>Ca to <sup>48</sup>Ca. Some of the scatter about the line on Figure 15 can be assigned to counting error in the electron probe analyses, and some may result from inhomogeneity caused by exsolution of Ti-bearing oxide. There is no evidence for a systematic bias with Fe/Mg ratio. For the olivine suite, Ti was detected by electron probe analysis for only four out of the seven samples, and the electron probe analyses correlated linearly with the ion probe analyses within the 2σ counting precision.

*Na*

Thorough analyses were made of Na in olivines from mantle-derived peridotites (Fig. 16). Although

the concentrations are too low for accurate electron probe analysis, there is a linear correlation with ion probe analyses within the 2σ counting error of the electron probe. Because of the small range of Fe/Mg, these samples do not allow testing of a possible matrix effect.

For olivines of Table 1 only sample 2 from a wehr-

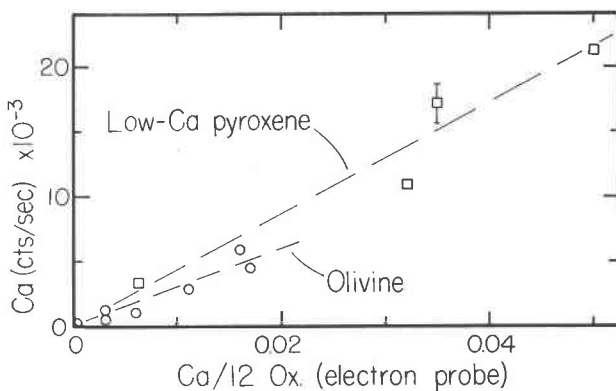


Fig. 8. Secondary ion yield for Ca<sup>+</sup> in low-Ca pyroxene compared to olivine. Data obtained during same analysis session. Vertical bar shows reproducibility of secondary ion count rate for 73-165 pyroxene during session.

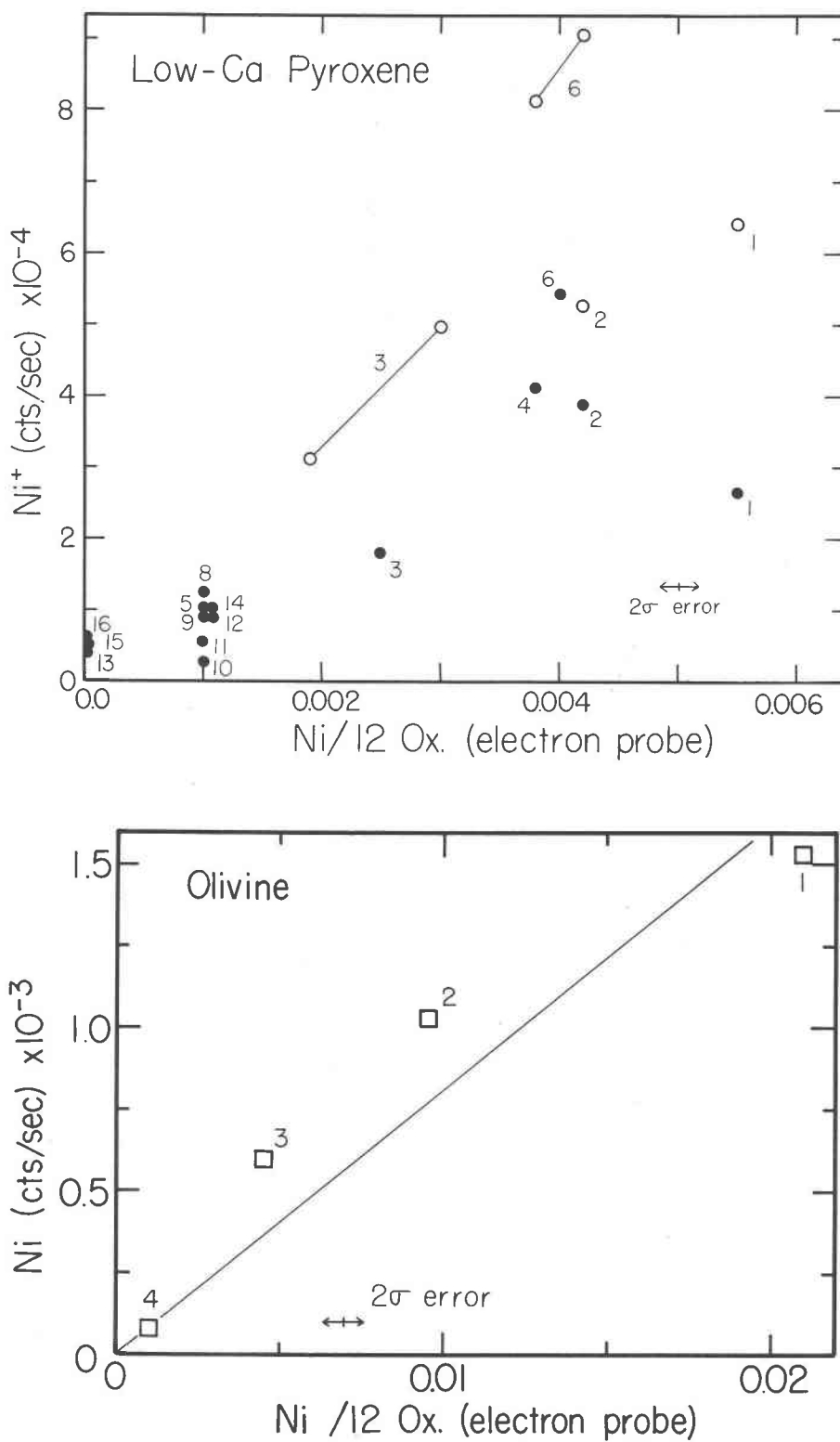


Fig. 9(a). Ni<sup>+</sup> secondary ion count rate vs. Ni cations /12 oxygens for low-Ca pyroxene. Open and solid symbols represent analyses made on different days. (b) Ni<sup>+</sup> secondary ion count rate vs. Ni cations /12 oxygens for olivine.

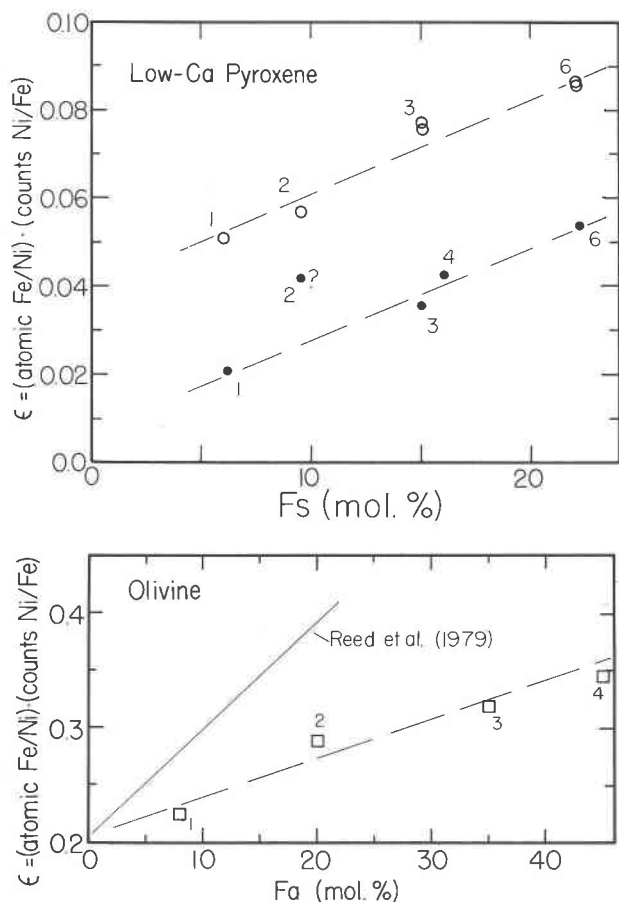


Fig. 10(a). Secondary ion yield factor for nickel ( $\epsilon$ ) vs. ferrosilite (Fs) content for Ni-rich, low-Ca pyroxenes, Symbols as in Fig. 9a. The cause of the anomalous position of the dot for specimen 2 is unknown. (b) Secondary ion yield factor for nickel ( $\epsilon$ ) vs. fayalite (Fa) content for Ni-rich olivines. Solid line is from Reed *et al.* (1979) adjusted to same intercept.

lite inclusion in basalt shows high (130 ppm) Na. Other olivines, all from rocks formed under near-surface conditions, have Na levels of near 1 ppm with a restricted range. With the exception of sample 1 of Table 2, electron probe analyses of low-Ca pyroxenes have insufficient precision to test for matrix effects. Assuming no matrix effects the ion probe count rates in Table 2 show no clear trend with *mg* although the highest values occur at intermediate *mg* as for several other elements.

#### Other elements (Li, K, Sc, V, Co)

Although these elements can be measured readily in most olivines and low-Ca pyroxenes by ion probe analysis, they are too low in concentration for the electron probe. A major effort will be needed to calibrate the ion-probe data by comparison with bulk

analyses of carefully selected homogeneous standards; particularly difficult will be testing for matrix effects. An approximate calibration can be obtained using the relative SI yields for other materials for which the concentrations of two elements are known. For example, the three adjacent transition elements Cr, V and Ti give approximately equal SI yields for pure metal targets (Storms *et al.*, 1977), and Cr in a pyroxene standard could be used as a semi-quantitative reference standard for V in pyroxenes. This assumes a similar relative yield in an oxide matrix.

Relative yield factors are a function of instrumental parameters as well as matrix. Because we have not determined sensitivity factors for our instrument, we rely on data of Meyer (1978), Storms *et al.* (1977), and Gittins *et al.* (1972). The relative SI yields of trace elements are now discussed and compared with observed trends, especially for several pyroxenes for which emission optical spectrographic analyses (Table 5a) are available (Howie, 1955).

Assuming that the SI yields for Ti and V are equal on an atomic basis, and not matrix dependent, 1550 cps for  $\text{Ti}^+$  corresponds to 840 ppm Ti (Fig. 15) and hence 860 ppmV. Thus 1 cps should correspond to 0.53 ppm. These estimates for five samples (Table 5b) are systematically low by  $\sim 2.2$ . Vanadium was detected in only two olivines in Table 1, and the 2 cps for sample 2 would correspond to  $\sim 1$  ppm if the pyroxene calibration is applicable to olivine.

Cobalt ion yields can be expected to be close to both Fe and Ni, but because high-resolution Fe data were not obtained, reference will be to Ni. Using the relative ion yields of Co to Ni as  $\sim 1.75$  for silicate glass (Meyer, 1978) and Ni data for sample 6 of Table 2 (544 cps  $\text{Ni}^+$  equals 710 ppm Ni), 1 cps corresponds to 0.73 ppm Co. The resulting estimates (Table 5b) are in the correct range but agree poorly in detail with Howie's (1955) data in Table 5a. The calculated Co values for samples with high *mg* are low while those for samples with low *mg* are too high; differential matrix effects might be responsible.

Scandium ion yields are about 1.5 times those of Ti (Gittins *et al.*, 1972), and 1 cps should correspond with 3 ppm Sc. Calculated data in Table 5b appear twice as high as values in Table 5a, but these latter ones are all close to detection. If the pyroxene calibration is carried over to olivine, the count rates in Table 1 correspond to 1.0–6.0 ppm. Scandium correlates with Fe in low-Ca pyroxenes (Deer *et al.*, 1978), and such a correlation is also implied for olivine.

Potassium has a very high yield of SI, and Meyer (1978) gives a yield about twice that of Na in feldspar

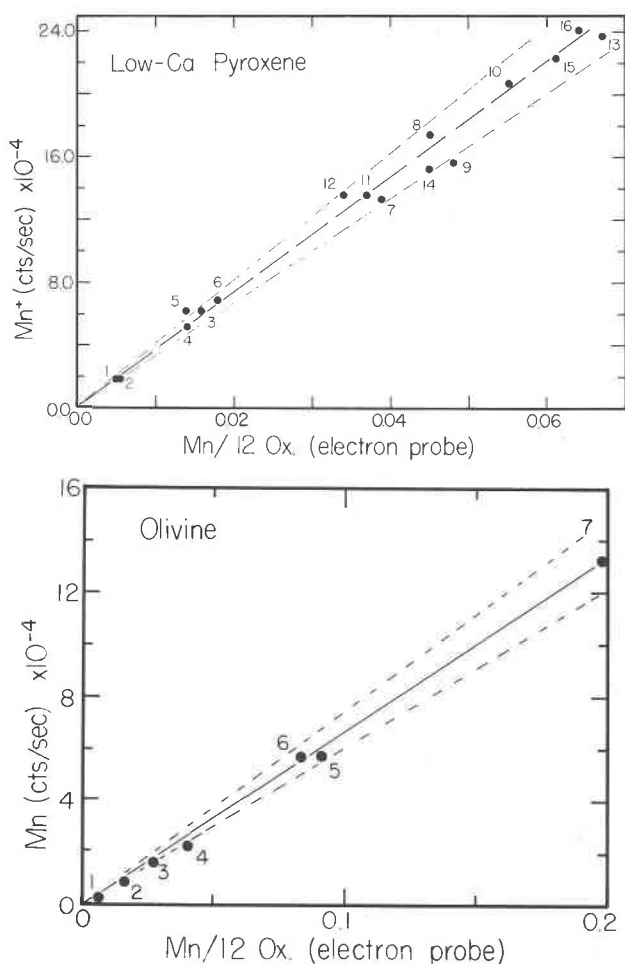


Fig. 11(a).  $Mn^+$  secondary ion count rate vs. Mn cations / 12 oxygens for low-Ca pyroxenes. Most points lie within  $\pm 10\%$  absolute dashed error limits about visual linear fit. (b)  $Mn^+$  secondary ion count rate vs. Mn cations / 12 oxygens for olivine.

matrix. For low-Ca pyroxene number 1, Table 2, 0.15 wt.%  $Na_2O$  corresponds to  $3.3 \times 10^5$  cps, and 1 ppm K should correspond to 300 cps. The resulting values of 1–2 ppm for the five low-Ca samples in Table 5 are  $\sim 10^3$  times lower than the emission spectrographic analyses. This very large discrepancy is best explained by impurities in the spectrographic analyses. Carrying over this calibration to olivine gives values of 30 to 100 ppb for K count rates of Table 1.

Lithium has a high SI yield about one-quarter that for Na (Meyer, 1978). For a plagioclase with known Li our instrument gives approximately 600 cps/ppm Li which is somewhat higher than that calculated from Meyer (1979). Using our Li calibration, data for 5 low-Ca pyroxenes (Table 5) are high relative to

those of Howie (1955) but not by a constant factor. Because the Li determinations of Howie are all near his detection limit of 5 ppm, further comparison is probably not warranted. Carrying over the calibration of 600 cps = 1 ppm to olivine yields 0.1–4 ppm (Table 1).

#### Discussion and prospects for ion microprobe analysis

Whereas the instrumentation for the ion probe is much more complex than for the electron probe, and sample preparation and analytical techniques are far more stringent, the ability to measure many trace elements at chosen points encourages further development of the ion probe. Even now, detection levels are quite satisfactory for many geochemical problems, and these levels can be improved at least 10-fold, and probably 100-fold, by improved design. Unlike elements with  $Z > 10$  in the electron microprobe, detection levels with the ion microprobe vary greatly from element to element depending mainly on: (a) the SI yield which varies by about  $10^5$ ; (b) the abundance of the measured isotope, and (c) whether high mass resolution is needed. The detection level can be estimated from the count rate in col. 6 of Table 4, and ranges from  $\sim 0.01$  ppm for alkali metals to  $\sim 1$  ppm for most transition metals. Even for Ni a detection level better than 10 ppm can be obtained, in spite of the weak yield of SI, and the need for high-resolution analysis with a low-abundance isotope.

Lower count rates result at high mass resolution because of attenuation of the transmitted beam by narrow slits. In the present AEI instrument, the intensity drops about 20-fold in adjusting from low to high resolution, mainly because of poor design of the

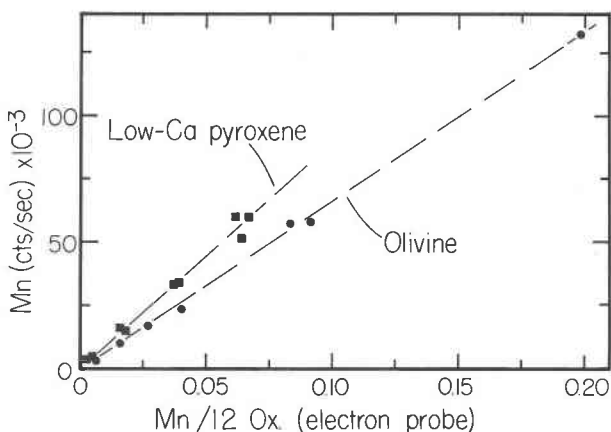


Fig. 12.  $Mn^+$  Secondary ion yield for low-Ca pyroxene compared to olivine. Data obtained during same analysis session.

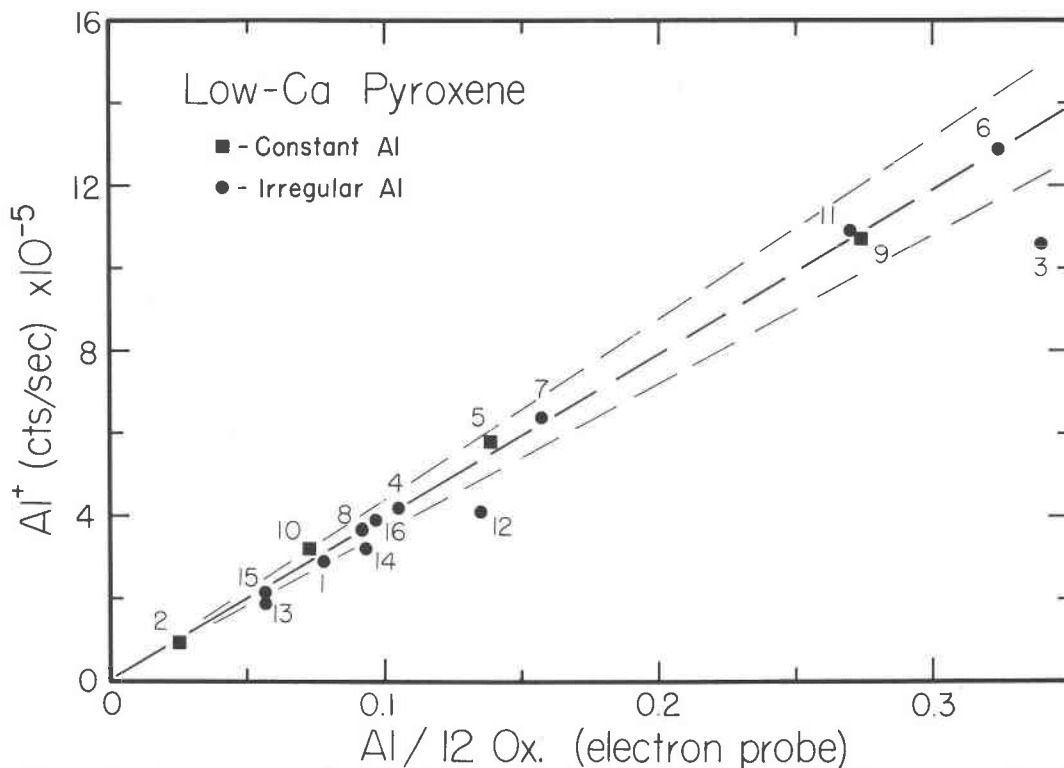


Fig. 13.  $Al^+$  secondary ion count rate vs. Al cations / 12 oxygens for low-Ca pyroxene. Linear fit includes most samples within  $\pm 10\%$  absolute error limits. Squares or circles, respectively, show samples found to be homogeneous or inhomogeneous by electron probe analysis.

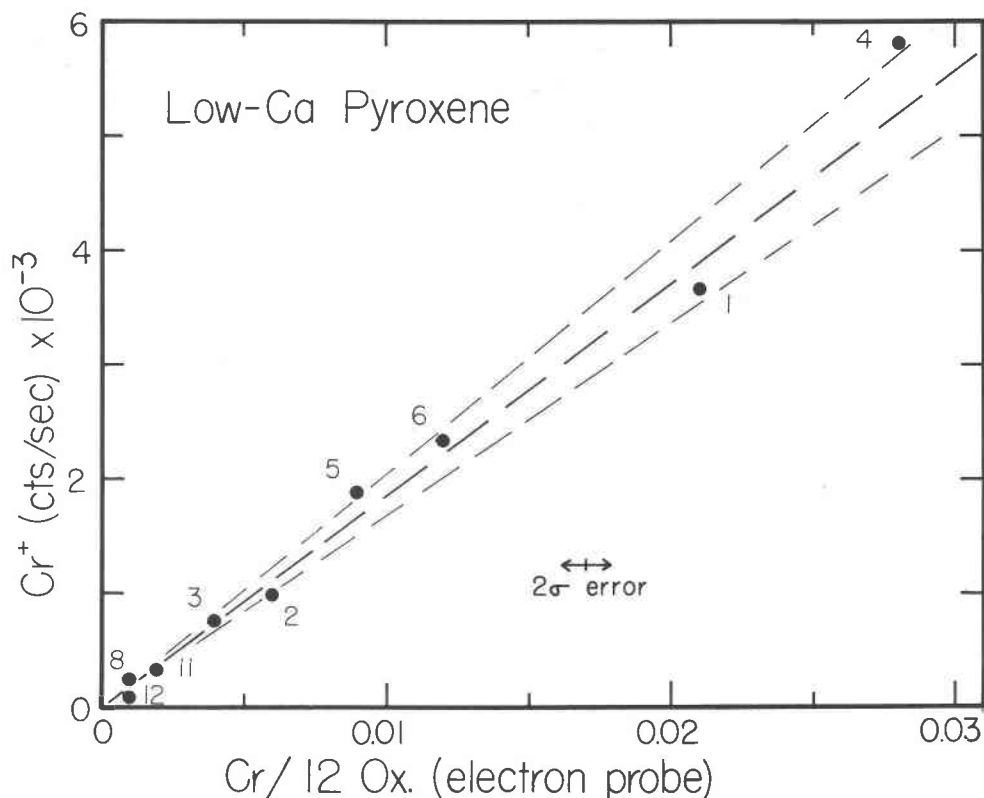


Fig. 14.  $Cr^+$  secondary ion count rate vs. Cr cations / 12 oxygens for low-Ca pyroxene.

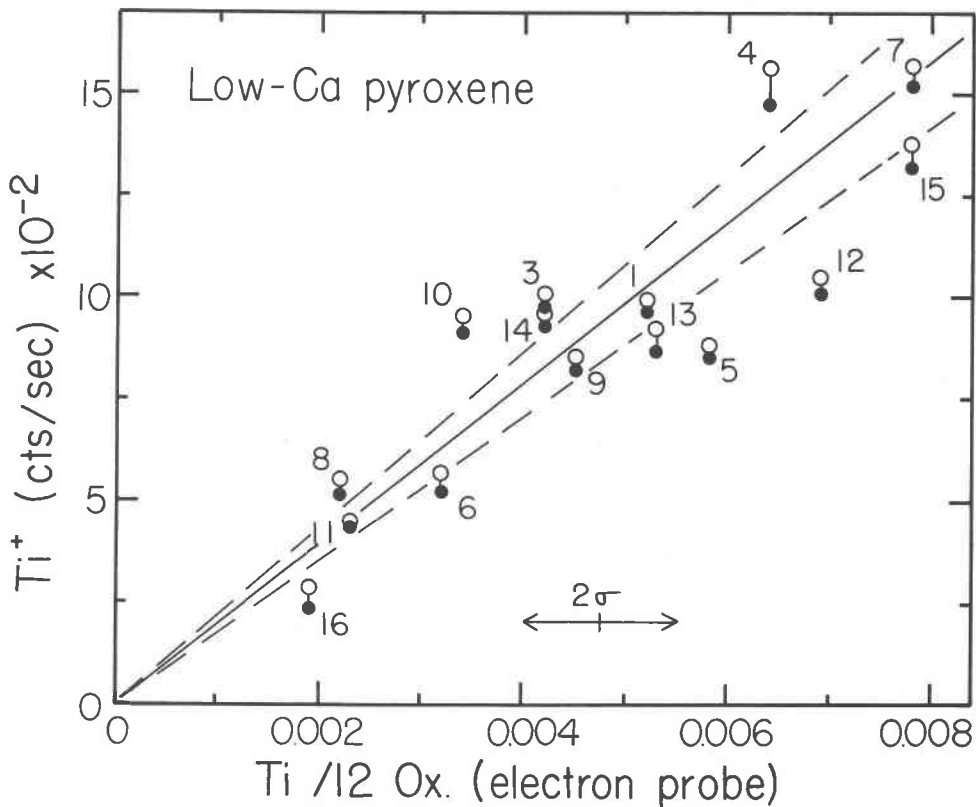


Fig. 15. Secondary ion count rate vs. cations/12 oxygens for titanium in low-Ca pyroxenes. Filled symbol is corrected for unresolvable  $^{48}\text{Ca}$  interference based on  $^{40}\text{Ca}$  count rate.

SI extraction optics. After modification by a design which should involve only a 3-fold decrease (Degréve *et al.*, 1979), the detection level for elements measured at high resolution should improve. Roughly speaking, the detection levels of most elements with  $Z > 10$  listed in Tables 1 and 2 are over a 100-fold better with the ion microprobe than the electron probe, especially for the alkali metals.

Now that the sensitivity problem has been solved, the major problem is to obtain accurate calibrations. The demonstration of a linear relation between SI signal and atomic concentration for some elements within one mineral type (*e.g.*, for Mn in orthopyroxene) is encouraging because it greatly simplifies quantitative procedures. However, the dependence of the SI yield of Ni on the Fe/Mg ratio of olivine and pyroxene provides a warning that a linear response should not be assumed unless necessary because of lack of appropriate standards. Furthermore the difference of calibration curves for olivine and pyroxene, even for an element whose response appears to be independent of Fe/Mg ratio (*e.g.*, Mn, Fig. 12), provides a second warning about casual use of stan-

dards. Currently there is no reliable quantitative theory for secondary-ion analysis, though a general theory (Andersen and Hinthorne, 1973) is valuable for semi-quantitative purposes (within a factor of 2?). Unfortunately it is at best tedious to assemble a set of reference standards for ion microprobe analysis, and at worst very difficult or even impossible for some elements. Ion probe users should exchange material to compare the response of the various instruments.

In spite of the problems, ion microprobe analysis of trace elements has an important role in future research in geochemistry, mineralogy, and petrology. Calibration problems are least difficult for minerals with near-identical or similar major-element chemistry, such as those from upper-mantle peridotites, and many important problems can be tackled. Minerals belonging to binary series can also be handled if standards can be assembled to test possible matrix effects, and again there are many important problems involving feldspars, olivines, and low-Ca pyroxenes. Minerals with complex compositional ranges, *e.g.*, garnets and amphiboles, will be difficult to handle unless a quantitative theory of SI emission can be de-

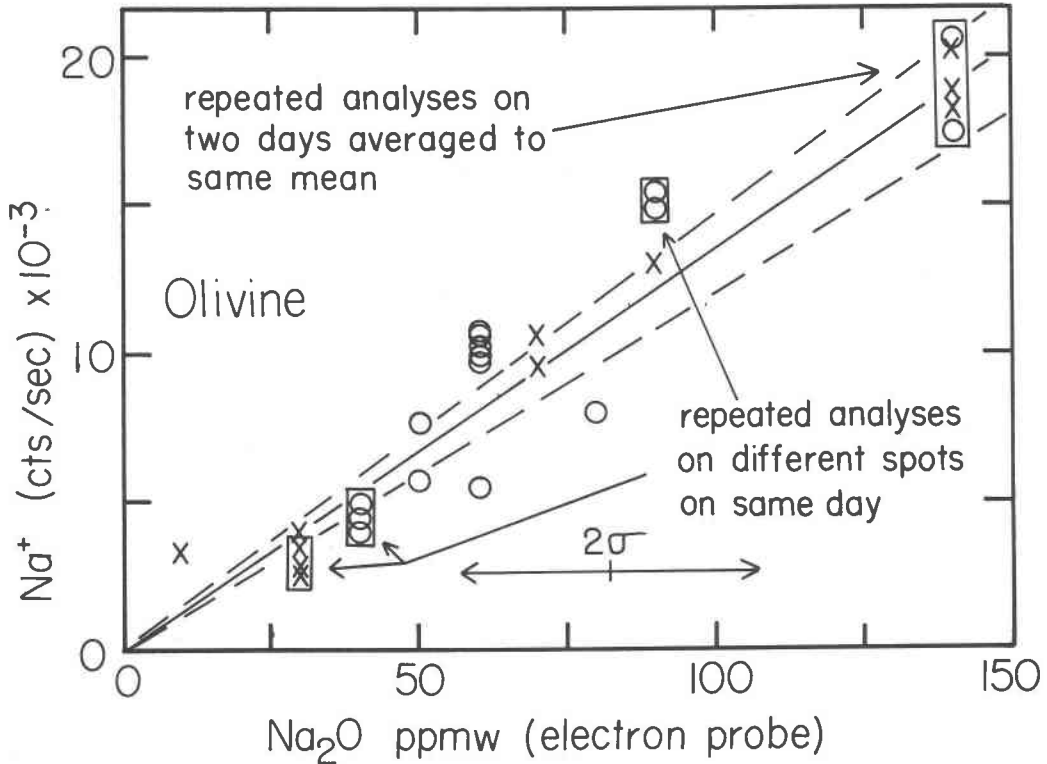


Fig. 16. Na<sup>+</sup> secondary ion count rate vs. Na ppm for olivines from mantle-derived peridotites. At these low concentrations, mole fraction is proportional to weight fraction. Round symbols and crosses are from different analysis sessions normalized to give the same mean count rate for Na-rich olivine 73-105.

veloped. Development of ion microprobe techniques for trace elements will be more difficult than of electron microprobe techniques for major and minor elements, but simultaneous use of both methods should

lead to major new results in geochemistry, mineralogy and petrology.

**Acknowledgments**

JVS wishes to point out that the analytical procedures were developed and the analyses obtained by the other authors. He and R. N. Clayton conceived the project of developing an ion microprobe with high mass-resolution capability for trace elements and isotopic ratios, in order to extend low mass-resolution studies. Recognizing that there would be difficulties with instrumental development and analytical procedures, the Earth Sciences Section of the National Science Foundation funded the project to test whether trace-element and isotope analyses would be feasible at high mass resolution. Only the AEI Company of Manchester, England, was then willing to attempt construction of a high-resolution ion microprobe. The subsequent instrument was modified considerably, and we are particularly indebted to T. Solberg, K. Dickens and R. Drais. The experience gained with similar instruments at Urbana, Illinois, and Cambridge, England, under the supervision of C. A. Evans and J. V. P. Long, respectively, was of great help. Since the original NSF grants (GA34131 and 35743; EAR 76-03604) the project has been supported equally by NSF grants (EAR 77-27100 and 78-23680) and NASA grants (14-001-169 and 14-001-171). The perseverance of John Hower (NSF) and Bevan French (NASA) in supporting the project during a black period of instrumental development was of critical value to final success. JVS wishes to record his personal gratitude to I. D. Hutcheon and I. M. Steele for their

Table 5. Analyses of trace elements in pyroxenes

Sample	*10	11	13	14	15
a) Emission spectrograph analyses (ppmw) of low-Ca pyroxenes (Howie, 1955).					
Li	3	5	2	4	3
Co	80	100	100	100	40
V	40	200	50	125	10
Sc	<10	<10	20	<10	15
K	4400	1300	-	600	1000
b) Ion microprobe analyses (ppmw)					
Li	4	13	8	4	11
Co	58	79	94	128	67
V	8	90	16	58	11
Sc	18	20	53	30	20
K	1	1.5	1	1.5	2

\*Sample number - see Table 2.

steady and skillful development of ion microprobe techniques over a long period when publishable results were rare.

## References

- Andersen, C. A. (1969) Progress in analytical methods for the ion microprobe mass analyzer. *International Journal of Mass Spectrometry and Ion Physics*, 2, 61–74.
- Andersen, C. A. and Hinthorne, J. R. (1973) Thermodynamic approach to the quantitative interpretation of sputtered ion mass spectra. *Analytical Chemistry*, 45, 1421–1488.
- Bakale, D. K., Colby, B. N. and Evans, C. A. (1975) High mass resolution ion microprobe mass spectrometry to complex matrices. *Analytical Chemistry* 47, 1532–1536.
- Banner, A. E. and Stimpson, B. P. (1975) A combined ion probe/spark source analysis system. *Vacuum*, 24, 511–517.
- Deer, W. A., Howie, R. A. and Zussman, J. (1978) *Rock Forming Minerals*, Vol. 2A, Single-Chain Silicates. Longman, London.
- Degrève, F., Figaret, R. and Laty, P. (1979) Depth profiling by ion microprobe with high mass resolution. *International Journal of Mass Spectrometry and Ion Physics*, 29, 351–361.
- Evans, C. A. (1972) Secondary ion mass analysis: a technique for three-dimensional characterization. *Analytical Chemistry*, 44, 67A–80A.
- Gittins, R. P., Morgan, D. V. and Dearnaley, G. (1972) The application of the ion microprobe analyzer to the measurement of the distribution of boron ions implanted into silicon crystals. *Journal of Physics D: Applied Physics*, 5, 1654–1663.
- Hervig, R. L. (1980) Minor and trace element composition of mantle minerals: Ca-Mg exchange between olivine and orthopyroxene as a geobarometer: origin of harzburgites. Ph.D. Thesis, University of Chicago.
- Herzog, R. F. K., Poschenrieder, W. P. and Satkiewicz, F. G. (1973) Observation of clusters in a sputtering ion source. *Radiation Effects*, 18, 199–205.
- Howie, R. A. (1955) The geochemistry of the charnockite series of Madras, India. *Royal Society of Edinburgh Transactions*, 62, 725–768.
- Howie, R. A. and Smith, J. V. (1966) X-ray emission microanalysis of rock-forming minerals. V. Orthopyroxenes, *Journal of Geology*, 74, 443–462.
- Liebl, H. (1975) Ion probe microanalysis. *Journal of Physics E: Scientific Instruments*, 8, 797–808.
- Long, J. V. P., Astill, D. M., Coles, J. N., Reed, S. J. B. and Charnley, N. R. (1980) A computer-based recording system for high mass-resolution ion-probe analysis. Eighth International Congress on X-ray Optics and Microanalysis, p. 316–321. Pendell Publishing Co., Midland, Michigan.
- Meyer, C. (1978) Ion microprobe analyses of aluminous lunar glasses: a test of the "rock type" hypothesis. *Proceedings Lunar and Planetary Science Conference 9th*, 1551–1570.
- Reed, S. J. B., Scott, E. R. D. and Long, J. V. P. (1979) Ion microprobe analysis of olivine in pallasite meteorites for nickel. *Earth and Planetary Science Letters*, 43, 5–12.
- Saxena, S. K. (1973) *Thermodynamics of rock-forming crystalline solutions*. Springer-Verlag.
- Shimizu, N. (1978) Analysis of zoned plagioclase from different magmatic environments: a preliminary ion-microprobe study. *Earth and Planetary Science Letters*, 39, 398–406.
- Shimizu, N., Semet, M. P. and Allegré, C. J. (1978) Geochemical applications of quantitative ion-microprobe analysis. *Geochemica et Cosmochimica Acta*, 42, 1321–1334.
- Simkin T. and Smith, J. V. (1970) Minor-element distribution in olivine. *Journal of Geology*, 78, 304–325.
- Smith, J. V. (1966) X-ray emission microanalysis of rock-forming minerals. II. Olivines, *Journal of Geology*, 74, 1–16.
- Steele, I. M., Hutcheon, I. D., Solberg, T. N., Smith, J. V. and Clayton, R. N. (1977a) Effect of energy selection on quantitative analysis in secondary ion microanalysis. *International Journal of Mass Spectrometry and Ion Physics*, 23, 293–305.
- Steele, I. M., Hutcheon, I. D., Solberg, T. N., Clayton, R. N. and Smith, J. V. (1977b) Ion microprobe analysis of plagioclase feldspars ( $\text{Ca}_x\text{Na}_{1-x}\text{Al}_{1+x}\text{Si}_{3-x}\text{O}_8$ ) for major and minor elements. *Proceedings Eighth International Conference on X-ray Optics and Microanalysis*, 180A–180F.
- Steele, I., and Hutcheon, I. (1979) Ion probe analysis of natural olivine: secondary-ion intensity variation and systematics for a simple binary silicate. In *Microbeam Analysis 1979*, Proceedings of the 14th Annual Conference of the Microbeam Analysis Society, 338–340.
- Steele, I. M., Hutcheon, I. D. and Smith, J. V. (1980) Ion microprobe analysis of plagioclase feldspar ( $\text{Ca}_{1-x}\text{Na}_x\text{Al}_{2-x}\text{Si}_{2+x}\text{O}_8$ ) for major, minor and trace elements. Eighth International Congress on X-ray Optics and Microanalysis, p. 515–525. Pendell Publishing Co., Midland, Michigan.
- Storms, H. A., Brown, K. F. and Stein, J. D. (1977) Evaluation of a cesium positive ion source for secondary ion mass spectrometry. *Analytical Chemistry*, 49, 2023–2030.
- Werner, H. W. (1975) Theoretical and experimental aspects of secondary ion mass spectrometry. *Vacuum*, 24, 493–504.

*Manuscript received, August 5, 1980;  
accepted for publication, January 5, 1981.*